



**HAL**  
open science

# Assessment of heat-induced errors in stereo-DIC measurements within the range of polymer thermoforming temperatures

Abderrahmane Ayadi, Dastidar Aniket, Lacrampe Marie-France

## ► To cite this version:

Abderrahmane Ayadi, Dastidar Aniket, Lacrampe Marie-France. Assessment of heat-induced errors in stereo-DIC measurements within the range of polymer thermoforming temperatures. Stereo-DIC, errors, uncertainties, heat haze, thermoforming, Association française de mécanique, Aug 2022, Nantes, France. hal-04063118

**HAL Id: hal-04063118**

**<https://imt-nord-europe.hal.science/hal-04063118>**

Submitted on 8 Apr 2023

**HAL** is a multi-disciplinary open access archive for the deposit and dissemination of scientific research documents, whether they are published or not. The documents may come from teaching and research institutions in France or abroad, or from public or private research centers.

L'archive ouverte pluridisciplinaire **HAL**, est destinée au dépôt et à la diffusion de documents scientifiques de niveau recherche, publiés ou non, émanant des établissements d'enseignement et de recherche français ou étrangers, des laboratoires publics ou privés.

See discussions, stats, and author profiles for this publication at: <https://www.researchgate.net/publication/363266596>

# Assessment of heat-induced errors in stereo-DIC measurements within the range of polymer thermoforming temperatures

Conference Paper · August 2022

CITATIONS

0

READS

8

3 authors:



**Aniket Ghosh Dastidar**  
IMT Lille Douai

6 PUBLICATIONS 1 CITATION

[SEE PROFILE](#)



**Abderrahmane AYADI**  
IMT Nord Europe

33 PUBLICATIONS 246 CITATIONS

[SEE PROFILE](#)



**Marie France Lacrampe**  
IMT Nord Europe

10 PUBLICATIONS 25 CITATIONS

[SEE PROFILE](#)

Some of the authors of this publication are also working on these related projects:



Hybrid experimental-numerical mechanics applied to thermoforming [View project](#)



Quantitative imaging [View project](#)

# Assessment of heat-induced errors in stereo-DIC measurements within the range of polymer thermoforming temperatures

A. GHOSH DASTIDAR<sup>a</sup>, A. AYADI<sup>a\*</sup> and M-F. LACRAMPE<sup>a</sup>

a. IMT Lille Douai, Institut Mines-Télécom, Centre for Materials and Processes, F-59000  
Lille, France

(\*) corresponding author: [abderrahmane.ayadi@imt-nord-europe.fr](mailto:abderrahmane.ayadi@imt-nord-europe.fr)

## Résumé:

*La présente étude traite des mesures de stéréo corrélation d'images numériques (stéréo-CIN) associées à des tests de corps rigides effectués dans la plage de thermoformage de polymères. En effet, la stéréo-CIN est récurrente en photomécanique pour mesurer des champs cinématiques. Néanmoins, en présence de panache thermique dans le chemin optique, tout changement de l'indice de réfraction de l'air provoque une distorsion des images optiques et par conséquent un manque de précision des mesures finales des déplacements. La procédure proposée vise à quantifier puis à filtrer les erreurs systématiques et le bruit induits par une convection thermique naturelle. Les vecteurs de déplacements mesurés ont d'abord été utilisés pour évaluer l'effet de la température et l'effet de la vitesse sur les erreurs systématiques et le bruit d'un système de stéréo-CIN préalablement calibré. Ensuite, une procédure de post-traitement a été proposée pour filtrer les erreurs de mesures. Un cas d'application a été considéré afin de démontrer que le filtrage temporel des erreurs systématiques, avec prise en considération du panache thermique, correspond à un gain de l'ordre de 44 %. Les résultats trouvés constituent une étape essentielle dans une démarche d'instrumentation d'un processus de thermoformage.*

## Abstract:

*The present study deals with stereo digital image correlation (stereo-DIC) measurements associated with rigid body tests performed within the temperature range of polymer thermoforming. Indeed, stereo-DIC is recurrent in photomechanics to measure kinematic fields. However, in the presence of a thermal haze in the optical path, any change in the refractive index of the air causes distortion of the optical images and consequently a lack of precision in the measured displacements. The proposed procedure aims to quantify and then filter out systematic errors and noise induced by natural thermal convection. The measured displacement vectors were first used to evaluate the effect of temperature and the effect of rigid-body displacement speeds on the systematic errors and the noise of a pre-calibrated stereo-DIC system. Then, a post-processing procedure was proposed to filter the measurement errors. An application case was suggested to demonstrate that temporal filtering of systematic errors with consideration of the thermal haze corresponds to an approximate gain of 44%. The found results constitute an essential step towards the instrumentation of a thermoforming process.*

**Mots clefs: Stereo-DIC, errors, uncertainties, heat haze, thermoforming.**

# 1 Introduction

Stereo-digital image correlation (stereo-DIC) is a metrological technique which has the potential to provide three-dimensional kinematic fields based on stereovision and digital image correlation algorithms [1,2]. The instrumentation approaches of open-mold forming processes constitutes one potential case of application of stereo-DIC to follow the mechanical deformations undergone by the material within “real” forming conditions. In the particular context of plug-assisted thermoforming process, the authors have demonstrated through previous works, the potential of stereo-DIC to: (i) map the final thickness fields of thermoplastic sheets [3] and (ii) to detect geometric instabilities during the stretching phase of softened and sagged thermoplastic sheets [4]. Despite these advantages of stereo-DIC, additional precautions are still necessary in order to avoid miss interpretations of the obtained kinematic fields. Indeed, the accuracy of the obtained measurements depends on the quality of the recorded optical images. However, the use of industrial thermoforming equipment is often associated with the presence of natural convective heat fluxes within the observation field of optical cameras. In the realm of experimental mechanics, various authors have worked on conducting DIC measurements in the presence of heat sources. When optical measurements are made at relatively high temperatures, *Yu et al.* reported three difficulties that affect the quality of the images of the speckle [5]. These difficulties are: (i) the saturation of image intensity due to radiative heat transfer mode, (ii) the degradation of image contrast due to speckle degradation and (iii) the distortion of images due to heat haze. Where, heat haze is a phenomenon which corresponds to the presence of a natural convective heat flux between hot and cold domains. When air is heated, local changes in its density and its index of refraction of light can result into non visually perceptible distortions of light beams recorded by optical cameras [6]. In the range of thermoforming temperatures of amorphous thermoplastic sheets (below 150 °C), *Yuile et al.* used CFD simulations to model the thermal field of a regulated thermal chamber to characterize the optical distortions during DIC measurements [7]. Their results demonstrated that in absence of any forced convective cooling, the measured deformation errors induced by heat haze cannot be neglected when air temperatures exceeded 60 °C. To quantify and then correct distortions of recorded optical images, *Ma et al.* proposed the use of the background-oriented Schlieren (BOS) technique and respectively the application of temporal averages on the corrected images before running the digital image correlation algorithms [8]. *Jones et al.* evaluated the attenuation of image distortions by imposing forced convective cooling in the field of view of optical cameras during the image acquisition phase and then by applying a temporal filter to the images before calculating the displacements [6]. The results from both previous studies proved that the application of temporal filters was the most effective solution to reduce distortions induced by heat haze.

The objective of the present study is to propose an alternative approach of quantify then correct the displacement errors after conducting image correlations. The proposed procedure relies on rigid body translation tests conducted on a tensile machine equipped with an auto-regulated heating chamber. The structure of the article is as follows: the experimental part is devoted to the experimental precautions to be considered in order: (i) to regenerate heat waves within the range of thermoforming temperatures of high impact polystyrene (HIPS) and (ii) to ensure temporal synchronization between the imposed and measured displacements while conducting the mechanical tests. The results and discussion part will focus on the temporal evolution of displacement errors under the effect of heat waves. The interest will be attributed to the effect of two parameters which are the regulation temperature and the displacement speed. The obtained results will be used to suggest a time filtering approach of measured displacements.

## 2 Material and methods

### 2.1 Equipment

Rigid body tests were carried out on a Roell Z010 tensile machine (Zwick<sup>®</sup>) equipped with pneumatic clamps, a 10 kN load cell. Temperature control was ensured by an auto-regulated thermal chamber (Zwick<sup>®</sup>), which was itself equipped with an observation door and an integrated convective fan to ensure homogeneous heat distribution. After the end of the thermal regulation phase, a type K thermocouple and an infrared camera (Optris<sup>®</sup>) were used to monitor the temperature inside the thermal chamber and the temperature of the sample respectively. A stereovision system (LaVision<sup>®</sup>) equipped with two CCD cameras of the type Imager MX-4M served to record speckle translations at a fixed frequency of 5 fps from outside the thermal chamber (see Fig.1.a). A white light source was used to illuminate the speckle patterns. All the rigid body motion tests used the same rectangular sample of 120×40×3 mm<sup>3</sup> and whose material was chosen to avoid geometric instabilities in the targeted temperature range ([105;120] °C).

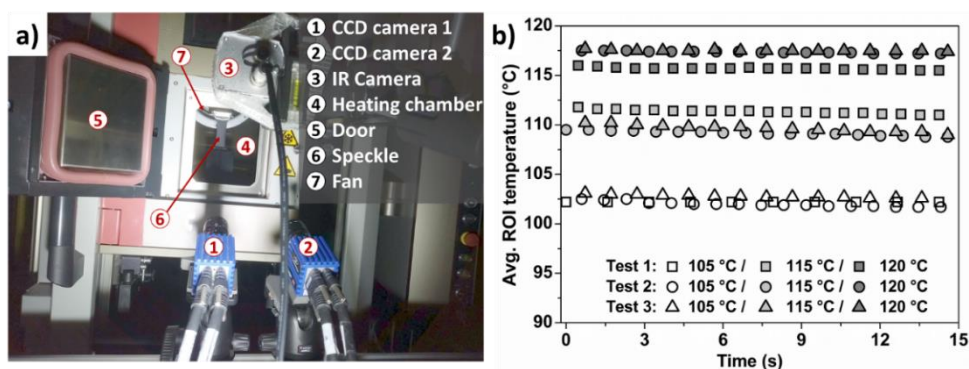


Fig. 1. (a) Experimental equipment. (b) Average temperature at the ROI measured by the IR camera.

### 2.2 Experimental procedure

Each of the rigid body tests respected the following steps: (i) Regulation of the thermal chamber, (ii) Stabilization of temperature (3 min), (iii) Triggering of stereovision recordings (5 fps), (iv) Opening of the observation door of the thermal chamber, (v) Stopping the ventilation of the thermal chamber, (vi) Starting the rigid body translation, (vii) Stopping all system after saturation of the random memories of the CCD cameras. It should be specified that the experimental procedure was conducted at three imposed speeds (10, 50 and 100 mm/min) and at four regulation temperatures (25, 105, 115 and 120°C). Where, the tests conducted at the same displacement speeds are respectively designated by Test1, Test2 and Test3 and the three highest temperatures are in the range of thermoforming temperatures of high impact polystyrene (HIPS). Given the random nature of image distortions by heat waves, one single rigid body test was deemed sufficient for each pair of parameters (speed, temperature). Despite the simplicity of the described experimental protocol, the synchronization of the measurements between the three systems (tensile machine, thermal chamber and stereo-DIC system) required additional precautions related to: (i) the temperature control during stereovision, (ii) the calibration of the stereo-DIC system and (iii) the identification of the reference state of the speckle patterns after temperature regulation. In the following paragraphs, a few details will be provided about these technical precautions.

#### 2.2.1 Temperature evolution during stereovision

The verifications were focused after the opening of the door of the heating chamber (i) to estimate the time duration required to maintaining the temperature above the glass transition of the HIPS (96 °C) and (ii) to characterize the temperature of the speckled region of interest (ROI) during stereovision recordings. In order to avoid significant decrease in temperatures between the start and the end of the optical measurements, the duration of all the digital image correlation calculations performed will be

truncated to 15 s duration after the start of effective sample translation. As indicated by Fig.1.b, the profiles of average temperatures measured at the speckled ROI exhibited a deviation of almost of 3 °C from each of the imposed regulation temperatures. In addition, by changing the regulation temperatures, the absence of overlapping domains between thermal profiles confirms that the heating chamber ensures relatively controlled performance during the stereovision measurements. As the CCD cameras were located relatively far from the heating chamber, thermal gradients oriented from the speckled ROI towards the camera lenses are assumed responsible of generation of heat haze.

## 2.2.2 Stereo-DIC calibration and post-processing

The calibration of the stereovision system was performed at 25 °C using a grid containing equidistant target points (Fig.2.a). Translations and rotations of the grid were performed in the plane (XY) of the hydraulic jaws of the traction machine to record five pairs of images. Using DaVis software (LaVision®) the intrinsic and extrinsic parameters of the stereo-DIC system were identified (Table 1). All image correlations considered a virtual gauge covering approximately  $35 \times 30 \text{ mm}^2$ . The defined extents of the subsets and of the step size were respectively fixed to  $19 \times 19 \text{ pixels}^2$  and 9 pixels. Due to the extent of final displacements reached by sample, an image correlation procedure implemented in DaVis and designated by sum-of-differentials was applied. More details about the sum-of-differentials procedure can be found in the following reference [3]

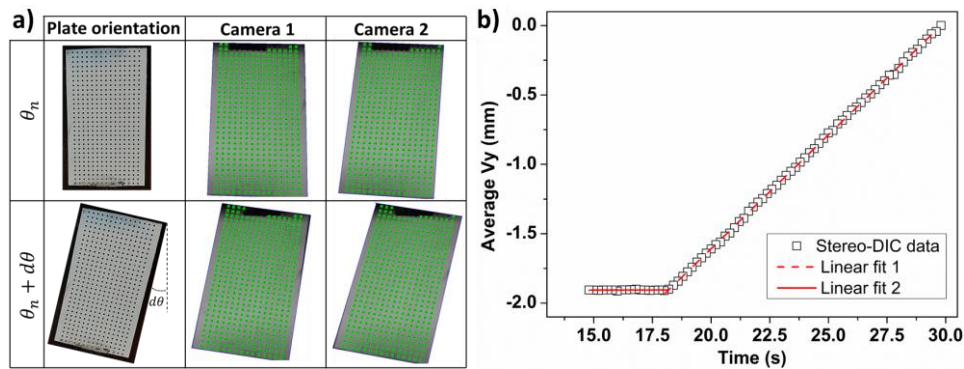


**Fig.2.** (a) Illustration of the calibration grid and the corresponding reference markers. (b) Backward double-fit identification of the reference of effective rigid body motions.

Before conducting the digital image correlations, it was necessary to objectively identify the reference state of the displacements at the start of the rigid body motion from the recorded sets of stereoscopic images. The considered method to identify the reference pair of images at the origin of times was based on post-processing the recorded images in a reversed order (from the end to the beginning). Then, based on a double linear fitting operations, the origin of time was identified at the point of intersection of the fitted curves. This two-step procedure was applied before for all tests. An illustrative example of this method is provided in Fig.2.b where negative displacements correspond to the reversed order post-processing of the stereoscopic images. Two domains can be identified: (i) the first is a quasi-static domain which corresponds to the lapse of time before the start of the effective translation of the speckled sample and (ii) the second corresponds to a quasi-linear increase of displacements at constant slope and which corresponds to the effective rigid motion.

**Table 1** Intrinsic and extrinsic parameters obtained from calibration of the stereo-DIC system

Parameters	Cam. 1	Cam. 2
Rotations (°)	37.034, -2.979, -2.157	36.014, 6.378, -0.854
Positions (mm)	-14.246, -195.191, 645.764	-22.327, -192.428, 653.943
Focal length (mm)	43.158	43.340
Scale factor (pixel/mm)	11.151	

### 2.2.3 Effect of reference state of displacements on statistical data

The influence of the choice of the reference state of the speckle on the statistical distribution of data was further checked at 25 °C (*i.e.* in absence of thermal haze). In this context, a first reference state (Ref1) was identified based on the double regression method (as defined in section 2.2.2) and a second reference state (Ref2) was defined visually at the moment of total opening of the window observation of the thermal chamber. Image correlation operations were then conducted on the same set of stereoscopic images corresponding to the rigid body test conducted at 10 mm/min and 25 °C. To visualize the distribution of displacements ( $V_y$ ) centered histograms were extracted at five time stamps which were defined at 1, 2, 3, 4 and 5 seconds from Ref1 and Ref2 respectively. In the case of Ref1 (Fig.3.a), the spatial distributions of the centered displacements seem to obey a single Gaussian distribution. However, in the case of Ref2 (Fig.3.b), the centered histograms indicate the presence of at least two types of displacements in the same ROI. Based on further visual inspections of the recorded pairs of stereoscopic images, it was confirmed that at the moment of opening of the chamber window and before the initiation of the rigid body translation, the ventilation fan was not completely stopped. Consequently, the observed second population of displacements was obtained by the image correlation algorithm due to the change of light reflection by the blades of the fan. The deceleration during time of the left side peaks in Fig.3.b. According to the highlighted challenges related to the visual choice of the reference state after thermal regulation, the double regression method was adopted to further quantify the haze induced errors as shall be discussed in the following sections.

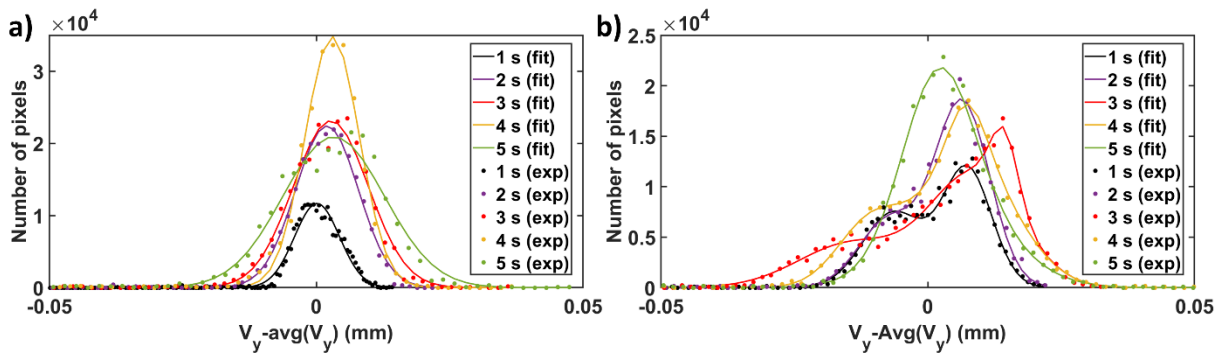


Fig.3. Histograms of centred  $V_y$  corresponding to Ref1 (a) and Ref2 (b)

### 2.2.4 Statistical analyses of temporal random errors and bias errors

In the current study, the quantification of the precision and errors of stereo-DIC was limited to the  $V_y$  components of displacement vectors. The focus was mainly attributed to the evaluation of the temporal random errors ( $T\_Stdev$ ) as expressed in Eq. 1 and of the bias errors  $BEr(t)$  as expressed in Eq. 2. The reader can refer to the following references to have more insight about the evaluation of noise and systematic errors from stereo-DIC measurements [8, 9].

$$T\_Stdev = \sqrt{\frac{1}{T} \sum_{t=1}^T \left[ (Vy_t - Vy_t^*) - \frac{1}{T} \sum_{t=1}^T (Vy_t - Vy_t^*) \right]^2} \quad (1)$$

Where,  $T$ ,  $Vy_t$  and  $Vy_t^*$  correspond respectively to the total time increments ( $T=75$ ), the measured and imposed displacement components at a time increment ( $t$ ).

$$BEr(t) = \left[ \frac{1}{N \times M} \sum_{i,j=1}^{N,M} (Vy_{ij}) \right]_t - Vy_t^* \quad | \quad t \in [1, \dots, 75] \quad (2)$$

Where,  $N$  and  $M$  are the total number of subset centres along the X and Y directions of the ROI.

### 3 Results and discussion

#### 3.1 Temporal random errors (Noise)

The evaluation of  $T\_Stdev$  maps was conducted with respect to the absence and then with presence of heat haze. As illustrated in Fig.4.a, the maximum noise level of measured displacements at 10 mm/min speed was relatively less than 0.02 mm through the entire ROI. By increasing the displacement speed to 50 and then 100 mm/min, the maximum noise levels increased up to 0.05 mm. Where the noise levels indicated a gradual increase from the top to the bottom of the ROI. On one hand, such observation can be attributed to the significant displacement translations of the speckle between consecutive recorded pairs of images with respect of the considered acquisition frequency. On the other hand, the observed vertical noise gradient can be due to a limited diffuse illumination of the speckle patterns from outside the heating chamber as can be observed from the shift of the greylevel histograms in Fig.4.d.

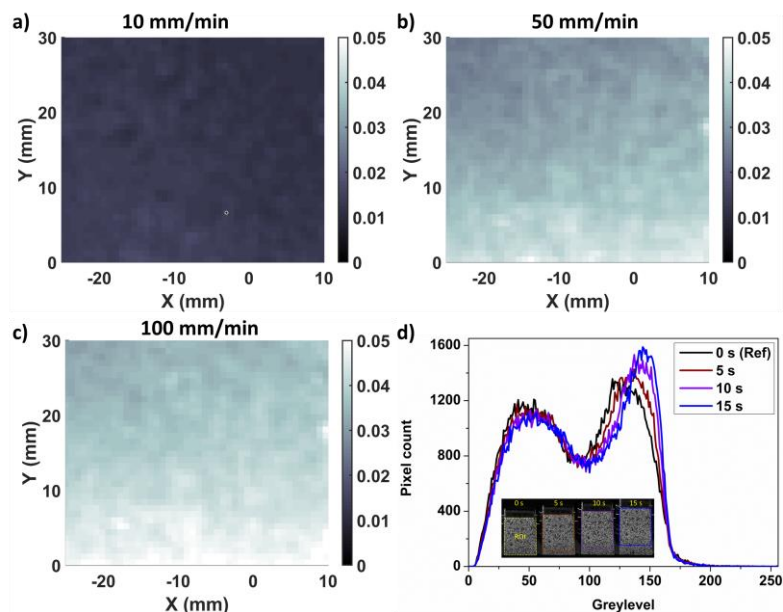


**Fig.4.** (a-c)  $T\_Stdev$  maps evaluated from tests conducted at 25 °C. (d) Greylevel distributions within the ROI for the test conducted at 25 °C and 100 mm/min

To highlight the effect of heat haze, the results corresponding to all the tests conducted at 10 mm/min were considered. Based on a comparison between the  $T\_Stdev$  at room temperature Fig.4.a and  $T\_Stdev$  maps obtained respectively at 105, 110 and 115°C, the spatial arrangements of noise exhibit local fluctuations (Fig.5). Such local effects traduce the noise induced by image distortions during the test duration due to the existence of thermal haze. Moreover, the higher was the regulation temperature of the heating chamber, the higher were the thermal gradients within the optical field of the stereoscopic system and thus, more significant levels of  $T\_Stdev$  were observed (Fig.5).

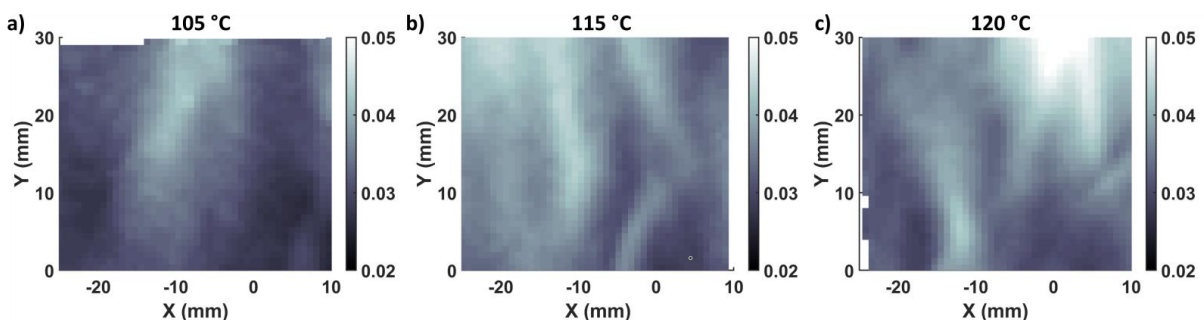


**Fig.5.**  $T\_Stdev$  maps evaluated from tests conducted at 10 mm/min



### 3.2 Time evolution of bias errors (systematic errors)

The time evolution profiles of displacement bias from all tests are reported in Fig.6.a. All profiles seem to obey to quasi-linear regression functions. In the absence of heating, the bias-error curves have negative slopes for all the tested displacement speeds which indicates an underestimation of the measured stereo-DIC displacements. Moreover, such systematic errors were more significant as the imposed displacement speeds increased. Indeed, the corresponding absolute values of the respective slopes increased from  $6 \times 10^{-3}$  to  $28.8 \times 10^{-3}$  and to  $51.1 \times 10^{-3}$ . By recalling that the number of numerical correlation operations is fixed to 75 iterations, this effect can be attributed to (i) the respective translation deviations of 0.16, 0.83 and 1.67 mm between the respective image pairs and to (ii) an accumulation of computational errors induced by the used correlation method. Under the effect of heat haze, the slopes of the measured displacement bias profiles decreased by approaching the zero line compared to the cases at 25 °C. Indeed, for speeds of 10 and 50 mm/min, the increase of temperature from 105, 115 to 120 °C seems to shift the evolution of the bias errors towards positive values. However, this observation was not the same at a speed of 100 mm/min particularly at 115 and 120 °C. Such an irregular change did not seem only related to the optical distortions induced by natural convection of air but it seemed also related to the onset of local turbulence of hot air at the interface of the moving sample at 100 mm/min.

### 3.2 Temporal filtering of bias errors

According to the considered experimental protocol, the global bias of the measured displacements can be broken down into an additive contribution of (i) systematic errors induced by the image correlation method in the absence of any heat haze and (ii) systematic errors induced by heat haze. The output results of thermally induced systematic errors are provided in Fig.6.b. The obtained results showed that the time-evolution of the haze-induced errors were quasi-linear with positive slopes. The corresponding linear regression curves can be considered as rectification functions of thermally-induced systematic errors.

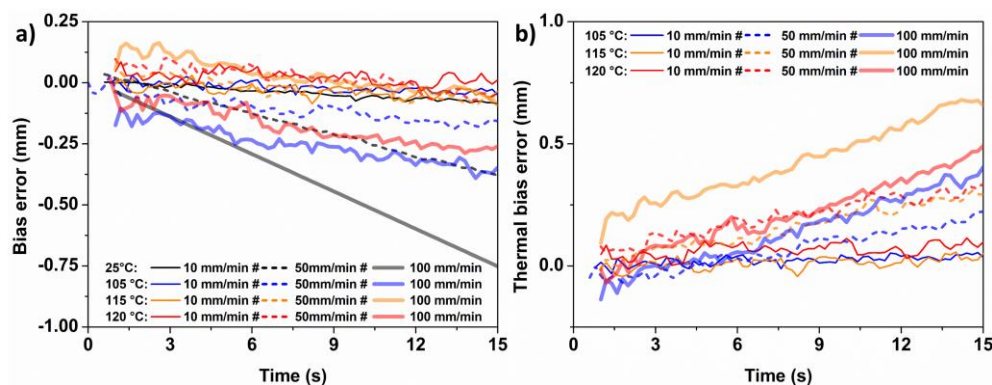
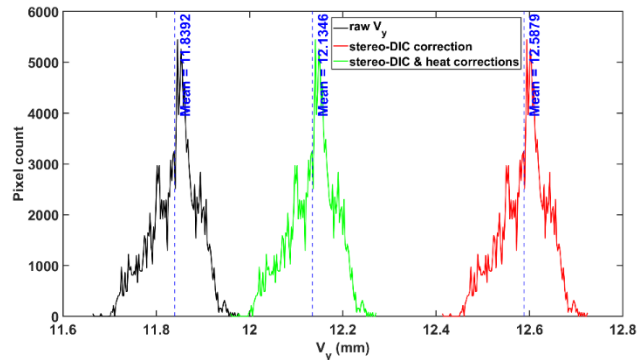


Fig.6. (a) Time evolution of global systematic errors. (b) Time evolution of thermal bias errors

### 3.3 Case application of temporal filtering of systematic errors

Based on the previously considered bias rectification functions, it was possible to define a temporal correction procedure by filtering the effect of heat haze. In order to illustrate this correction procedure, a time stamp at 15 s was considered from the displacement data of the rigid body motion test carried out at 120 °C and at a speed of 50 mm/min. First, the imposed displacement recorded by the tensile machine was retrieved from the stereo-DIC displacements to assess the spatial distribution of the global bias errors (Fig.7). Then the bias errors estimated at 25 °C and 50 mm/min for the same time stamp were removed. The histograms of displacements corresponding to the output of both previous operations are reported in Fig.7 and their respective mean displacement values correspond to 11.839 and 12.588 mm. Finally by further subtracting the amount of thermal haze based on the rectification function

corresponding the considered test (120°C and 50 mm/min), the mean displacement value shifted to 12.134 mm. Before making any corrections the displacement errors represented 5.29 % of the imposed displacement and after conducting previously indicated filtering operation, the relative error was reduced to 2.23 %, which corresponds to an approximate gain of 44.6 %.



**Fig.7.** Histogram distributions illustrating the effect of filtering global systematic errors and thermal haze induced systematic errors

## 4 Conclusion

The main conclusions of the current study are related to the assessment of systematic errors and noise based on rigid body tests conducted within the range of thermoforming temperatures. First, the experimental verifications confirmed the necessity to check the performance of the heating chamber and to objectively identify the reference state of the displacements. Second, the assessment of temporal random errors indicated a sensibility of noise to the illumination quality as highlighted at 25 °C and by changing the displacement speeds. In presence of heat haze, the noise distributions indicated the existence of local fluctuations which were increased as the regulation temperature was elevated. Third, the time evolution of systematic errors at 25 °C indicated a dependence of the imposed displacement speed. However, within the range of the considered temperatures the systematic errors were reduced as was indicated by a change of the slopes of the bias error profiles. However, at a speed of 100 mm/min, unusual change of the bias errors was hypothetically explained by a potential presence of turbulent convective effect of hot air in addition to the natural convection. By assuming additive decomposition of systematic errors into errors induced by the stereo-DIC measurements in absence of heat sources and errors induced by heat haze, a temporal correction scheme has been proposed. According to the considered case of application such correction procedure was able to enhance the precision of measured displacements by approximate gain of 44 %. In addition to these obtained results, further work is still required (i) to shed more light of convective heat turbulence at displacement speeds higher than 100 mm/min and (ii) to extrapolate the correction procedure to high-temperature stretching tests of thermoformable polymers.

## Acknowledgements

The authors acknowledge the European Regional Development Fund FEDER, the French state and the Hauts-de-France Region council for co-funding the PhD grant of Mr. Aniket GHOSH DASTIDAR.

## References

- [1] Y. Wang, P. Lava, S. Coppieters, P. V. Houtte, D. Debruyne, Application of a multi-camera stereo dic set-up to assess strain fields in an erichsen test: methodology and validation, *Strain*. 49 (2013) 190–198.

- [2] P. Duchene, S. Chaki, A. Ayadi, P. Krawczak, A review of non-destructive techniques used for mechanical damage assessment in polymer composites, *J. Mater. Sci.* 53 (2018) 7915–7938.
- [3] A. Ayadi, M.F. Lacrampe, P. Krawczak, Bubble assisted vacuum thermoforming: considerations to extend the use of in-situ stereo-DIC measurements to stretching of sagged thermoplastic sheets, *Int. J. Mater. Form.* 13 (2020) 59–76.
- [4] A. Ayadi, M.F. Lacrampe, P. Krawczak, A comprehensive study of bubble inflation in vacuum-assisted thermoforming based on whole-field strain measurements, in: *AIP Conference Proceedings*, AIP Publishing LLC, 2018, pp. 120004.
- [5] L. Yu, B. Pan, Overview of high-temperature deformation measurement using digital image correlation, *Exp. Mech.* 61 (2021) 1121–1142.
- [6] E.M.C. Jones, P.L. Reu, Distortion of digital image correlation (DIC) displacements and strains from heat waves, *Exp. Mech.* 58 (2018) 1133–1156.
- [7] A. Yuile, R. Schwerz, M. Roellig, R. Metasch, S. Wiese, Heat haze effects in thermal chamber tensile tests on digital image correlation, in: *19th Int. Conf. Therm. Mech. Multi-Physics Simul. Exp. Microelectron. Microsystems*, IEEE, 2018, pp. 1–7.
- [8] M. Chang, Z. Zhoumo, Z. Hui, R. Xiaobo, A correction method for heat wave distortion in digital image correlation measurements based on background-oriented Schlieren, *Appl. Sci.* 9 (2019) 3851.
- [9] A. Ghosh Dastidar, Modelling and simulation of thermoforming, Thesis, Université Lille I, 2022.